Second- and third-harmonic generation in birefringent photonic crystals and microcavities based on anisotropic porous silicon

I. V. Soboleva,[a] E. M. Murchikova, A. A. Fedyanin,[b] and O. A. Aktsipetrov
Department of Physics, M. V. Lomonosov Moscow State University, 119992 Moscow, Russia

(Received 14 June 2005; accepted 22 September 2005; published online 6 December 2005)

One-dimensional anisotropic photonic crystals and microcavities based on birefringent porous silicon are fabricated. The reflectance spectra demonstrate the presence of photonic band gap and microcavity modes with spectral positions tunable upon the sample azimuthal rotation around its normal and/or rotation of polarization plane of incident light. Simultaneous enhancement of second- and third-harmonic generation at the photonic band-gap edge due to the phase matching is observed. The angular positions of the second- and third-harmonic peaks are controllable via the anisotropy of the refractive indices of porous silicon layers. © *2005 American Institute of Physics*.
[DOI: 10.1063/1.2133910]

One of the potential applications of silicon-based photonic crystals in optoelectronics and intergrated optics is the fabrication of silicon compatible photonic devices.[1] Recently, significant progress has been achieved in the fabrication of silicon-based photonic band gap (PBG) structures of different dimensionality mostly using the wet etching accompanied by the photolithography or focused-ion-beam drilling.[2,3] Apart from intensive studies of linear optical properties of silicon photonic crystals, this generated much interest in their nonlinear properties as well. For example, ultrafast tuning of the band edge of silicon photonic crystals due to the third-order optical susceptibility has been observed recently.[4,5] The efficient up-conversion, such as second- and third-harmonic generation (SHG and THG), has also been demonstrated as a result of the enhancement of photonic density of states and giant dispersion at the PBG edge. The effective fulfilment of the phase-matching conditions obtained as the fundamental radiation is tuned across the long-wavelength PBG edge leads to the manyfold increase of the second-harmonic (SH) (Ref. 6) and third-harmonic (TH) (Ref. 7) intensities. Birefringence, which is directly attributed to the optical anisotropy of the medium, can also effectively control the up-conversion gain using the different dispersion properties of ordinary and extraordinary waves. The fabrication of silicon photonic crystals possessing birefringence[8–10] can open up prospectives to applications for integrated optics and on-chip devices of nonlinear photonics requiring the controllable manipulation of the up-conversion efficiency. Silicon crystal is isotropic due to the cubic lattice, but porous modification of silicon can exhibit a strong in-plane anisotropy of the refractive index due to shape anisotropy of Si nanocrystals and voids assembling the material.[11] This form anisotropy is achieved by etching of the (110) silicon wafers and introduced by the selective crystallographic pore orientation in equivalent [010] and [100] directions.

In this article, the simultaneous SHG and THG enhancement is studied in one-dimensional photonic crystals fabricated from the birefringent porous silicon when the fundamental radiation is tuned across the PBG edge. The angular positions of the SHG and THG peaks and the maximal intensity enhancement are shown to be controllable via the artificial birefringence of the porous silicon layers possessing an optical axis along the [001] direction.

Samples of anisotropic photonic crystals and microcavities are fabricated by electrochemical etching of p^+-type silicon wafers of the 50 mΩ cm resistance with (110) surface orientation in 22% hydrofluoric (HF) aqueous solution with ethanol. Porous silicon layers of different porosity and optical thickness are obtained by variation of the current density and the etching time. Refractive indices of porous layers are determined from reflectance spectroscopy of single porous silicon layers. Photonic crystals consist of 24 pairs of porous silicon layers with refractive indices of $n_1 \cong 1.81$ and $n_2 \cong 2.18$, respectively, and optical thickness of $\lambda_0/4$, where λ_0 is the wavelength corresponding to the PBG center at the normal incidence. Microcavities are made of two Bragg reflectors of 12 pairs of porous silicon layers separated by a $\lambda_0/2$-thick cavity spacer. Coupled microcavities have two spacers separated by additional intermediate Bragg reflector of three porous layers. Refractive index anisotropy of porous layers used is determined to be $\Delta n_1 \cong 0.03$ and $\Delta n_2 \cong 0.04$, respectively.

The output of the YAG:Nd^{3+} laser with wavelength of 1064 nm, pulse duration of 10 ns with energy of 6 mJ per pulse and spot diameter of 1 mm is used as the fundamental radiation for SHG and THG k-domain (angular) spectroscopy.

Birefringence of photonic crystals manifests itself in the dependence of the reflectance on the mutual orientation of the fundamental field polarization vector **E** and the main plane formed by the wave vector and the optical axis of photonic crystal. It is probed by rotation of **E** with the fixed main plane or by the changing of the main plane orientation keeping fixed the light polarization. Figure 1(a) shows the reflectance spectra of porous silicon microcavity measured for two values of the azimuthal angle ψ between the optical axis and the plane of incidence with $\psi=0°$ corresponding to the coincidence of the incident and $(1\bar{1}0)$ planes. Reflectance increases up to 0.9 in the range from 780 to 900 nm corresponding to the PBG and has a dip near 830 nm related to the microcavity mode. The spectral shift of the PBG and microcavity mode under sample azimuthal rotation is about 10 nm.

[a]Electronic mail: irina@shg.ru
[b]Electronic mail: fedyanin@shg.ru

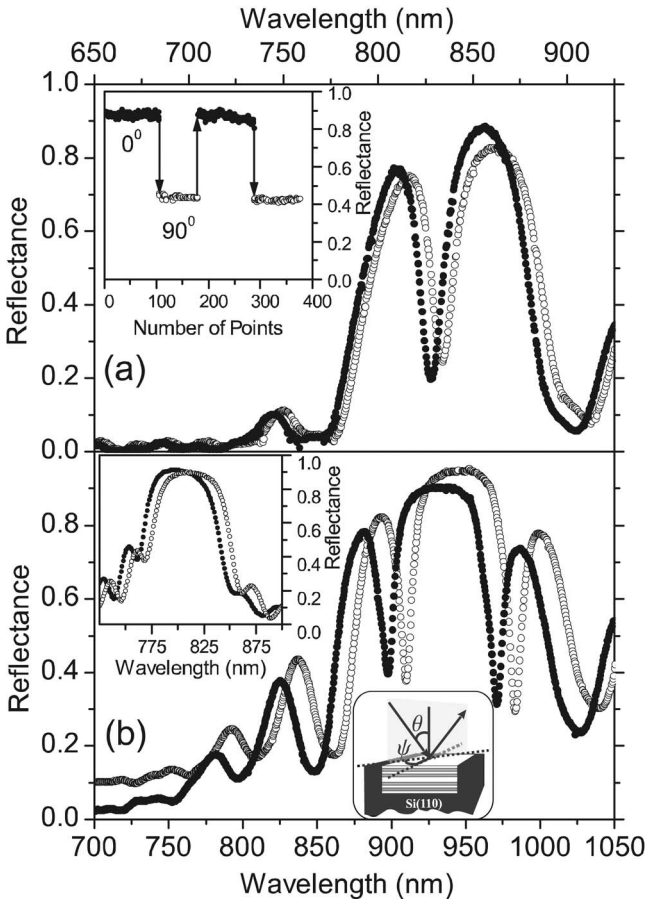

FIG. 1. (a) Spectra of reflectance of the *s*- (open circles) and *p*- (filled circles) polarized light from the anisotropic microcavity with $\lambda_0=860$ nm measured for $\psi=90°$. Inset: The reflectance contrast measured for *s*-polarized microcavity mode at $\psi=90°$ upon sample rotation to $\psi=0°$. Angle of incidence is $\theta=20°$. (b) The spectra of reflectance of the *s*-polarized light from the anisotropic coupled microcavity with $\lambda_0=960$ nm measured for $\psi=0°$ (filled circles) and $\psi=90°$ (open circles). $\theta=20°$. Inset: The spectra of reflectance of *s*-polarized light from the anisotropic Bragg reflector measured for $\psi=0°$ (filled circles) and $\psi=90°$ (open circles).

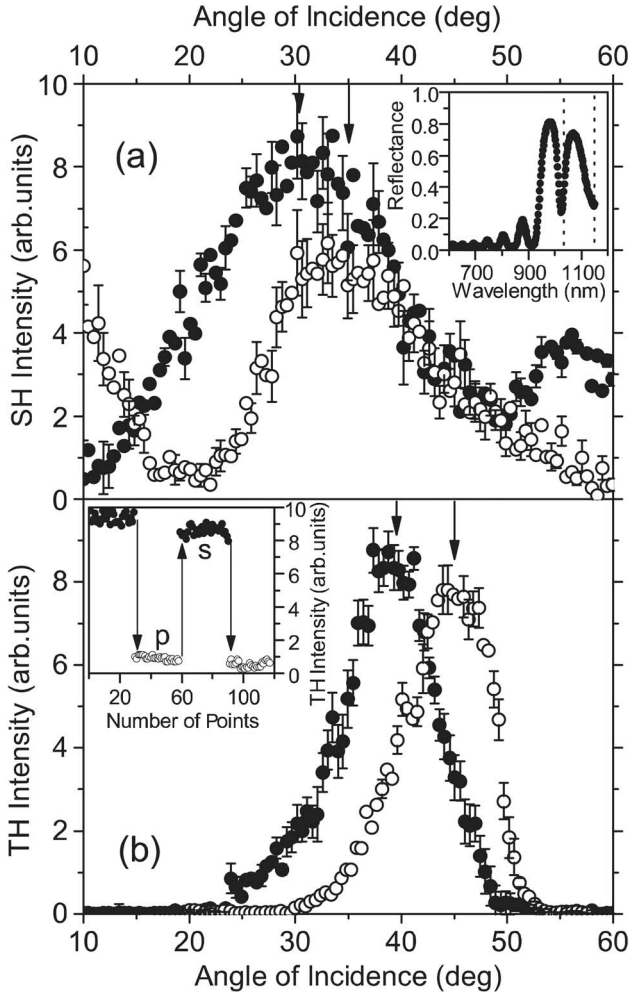

FIG. 2. (a) The SH intensity angular spectra of the microcavity with $\lambda_0=1100$ nm for the *s*- (filled circles) and *p*-polarized (open circles) fundamental wave. Arrows emphasize the angular shift of the SHG maxima. Inset: Reflectance spectrum of this microcavity. Band shows the part of the spectrum corresponding to the angular tuning range. (b) The TH intensity angular spectra of this microcavity for the *s*- (filled circles) and *p*-polarized (open circles) fundamental wave. Inset: The contrast of the TH magnitude measured for *s*- and *p*-polarized fundamental wave, $\theta=37°$.

The same spectral shift is obtained for reflectance spectra of the anisotropic photonic crystal presented in the inset of Fig. 1(b). This indicates that anisotropic photonic crystals and microcavities can be considered as uniaxial negative birefringent media with the optical axis along the [001] direction in the surface plane. The PBG and microcavity-modes shifts are also observed in anisotropic coupled microcavities shown in Fig. 1(b).

Figures 2(a) and 2(b) show the angular spectra of the SH and TH intensities, respectively, measured at $\psi=0°$. The SHG spectra have peaks at $\theta=31°$ and $\theta=35°$ with half-width at half-maximum (HWHM) about 10°. The THG spectra have peaks at $\theta=39°$ and $\theta=44°$ with HWHM about 5°. The SHG and THG enhancement by two and three orders of magnitude in comparison with signal out of PBG, respectively, is achieved at the long-wavelength PBG edge. The largest contrast in the TH intensity is shown in the inset of Fig. 2(b). Rotation of polarization of the fundamental wave leads to the 10-times changing in the TH intensity.

The SHG and THG enhancement results from the fulfilment of the phase matching conditions at the PBG edge of photonic crystals and microcavities. The coherency length of SHG and THG in the studied samples of total thickness of 9 μm is about 1.5 μm and 200 nm, respectively. The angular position of the intensity maxima in the SHG and THG spectra can be found using the phase matching conditions for fundamental and harmonic wave vectors projections on the periodicity direction in the reflection geometry written in the form

$$k_z^{(2\omega)} + 2k_z^{(\omega)} = 2G, \quad k_z^{(3\omega)} + 3k_z^{(\omega)} = 3G, \tag{1}$$

where $G=2\pi/d$ is the reciprocal vector of Bragg reflectors, and d is thickness of a period. The angular shift of the SHG and THG peaks for different polarization of fundamental light is associated with the in-plane anisotropy of refractive indices of the layers. The difference between the SHG and THG peak positions attributes to different phase mismatch to be compensated by the group velocity dispersion at the PBG edge. For calculation of the porous silicon effective refractive indices at the fundamental wavelength, reflectance spectroscopy of single porous layers and the dependences of mode spectral position on the angle of incidence and azimuthal angle are used. Figure 3(a) shows the microcavity mode shift $\Delta\lambda$ in the units of the mode HWHM Δ as a function of azimuthal angle ψ, where Δ of 9 nm is a constant

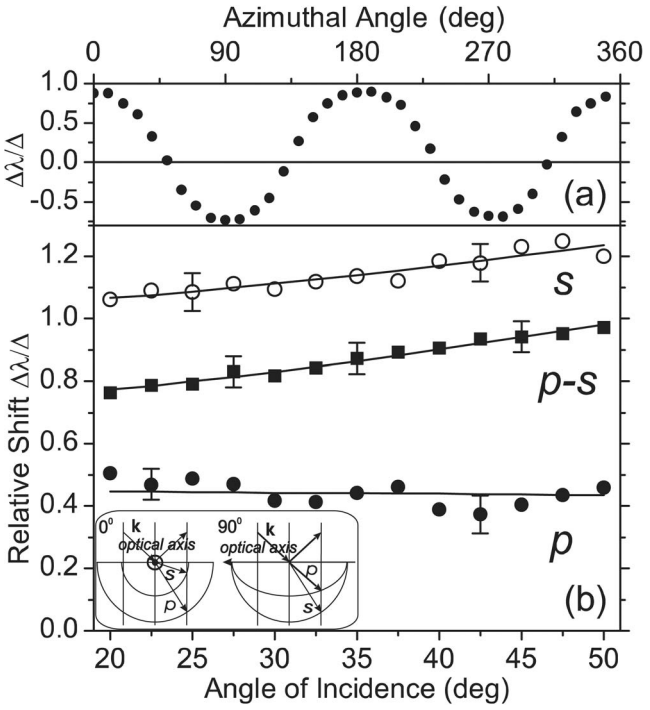

FIG. 3. (a) Dependence of relative shift of the microcavity mode position from *s*- to *p*-polarization on the sample azimuthal rotation for $\theta=40°$. (b) The angular dependences of mode relative shift measured for the sample rotation from $\psi=0°$ to $\psi=90°$ for *s*- and *p*-polarized modes (open and filled circles, respectively) and for polarization rotation from the *s* to *p* at $\psi=0°$ (filled squares). Curves are the fit within uniaxial birefringent crystal model.

for changes of ψ. The shifts have the same absolute values for $\psi=0°$, 90°, 180°, 270°, but signs of the shifts are different for the orthogonal azimuthal positions since the sample rotation leads to a change of the refractive index of the incidence wave from ordinary to extraordinary one. Figure 3(b) shows the angular dependences of $\Delta\lambda/\Delta$. Dependences are measured for the sample rotation from $\psi=0°$ to $\psi=90°$ in the *s*- and *p*-polarization (cases 1 and 2) and for polarization rotation from *p* to *s* with $\psi=0°$ (case 3). The relative shift $\Delta\lambda/\Delta$ of the *s*-polarized mode is maximal and reaches 1.2. The inset of Fig. 3(b) shows a cross-section of ellipsoids of refractive indices at *s*- and *p*-polarized waves for $\psi=0°$ and $\psi=90°$. The angular dependence of refractive index anisotropy $\Delta n(\theta)$ is a constant for cases 1 and 3 and has the ellipse arc shape for case 2. The $\Delta\lambda(\theta)$ dependence is a result of the dependence $\Delta n(\theta)$ and the blueshift of the mode wavelength for the oblique incidence $\lambda(\theta)=\lambda_0(1-(\sin\theta/n_{\mathrm{MC}})^2)^{1/2}$. Using

$$\Delta\lambda(\theta)=d_{\mathrm{MC}}((n_o^2-\sin^2\theta)^{1/2}-(n_e^2-\sin^2\theta)^{1/2}) \quad (2)$$

for cases 1 and 3 and

$$\Delta\lambda(\theta)=d_{\mathrm{MC}}(n_o^2-\sin^2\theta)^{1/2}(1-n_e/n_o) \quad (3)$$

for case 2, the main refractive indices $n_o(\omega)\cong 2.21$ and $n_e(\omega)\cong 2.17$ and the thickness $d_{\mathrm{MC}}\cong 195$ nm of the cavity spacer are obtained. The refractive indices of porous silicon layers at the SH and TH wavelengths estimated within the effective medium approximation are shown in Table I. Angular positions of the SHG and THG peaks calculated using expression (1) are $\theta^s_{\mathrm{SH}}=31°$ and $\theta^p_{\mathrm{SH}}=36°$; $\theta^s_{\mathrm{TH}}=39°$ and $\theta^p_{\mathrm{TH}}=44°$, respectively, and in a good agreement with the experimental values.

TABLE I. Main refractive indices of porous silicon layers at the TH, SH, and fundamental wavelengths.

Wavelength (nm)	n_{2e}	n_{1e}	n_{2o}	n_{1o}
355	2.53	1.91	2.56	1.94
532	2.34	1.91	2.38	1.94
1064	2.17	1.81	2.21	1.84

In conclusion, the enhancement of second- and third-harmonic generation is achieved in birefringent silicon-based photonic crystals and microcavities at the long-wavelength PBG edge due to anisotropy of dielectric function of porous silicon. Angular positions of the SHG and THG peaks coinciding with that calculated using phase matching conditions are shown to be shifted for different polarizations of the fundamental wave due to artificial birefringence in porous silicon layers. The results offer a practical means of controlling the simultaneous enhancement of SHG and THG in photonic crystals utilizing the combination of dispersion relations at the PBG edge and birefringence that can be useful for silicon-compatible devices of integrated optics.

This work was supported by the Russian Foundation for Basic Research, the Presidential Grant for Leading Russian Scientific Schools, and INTAS Grant No. 03-51-3784.

[1] A. Blanco, E. Chomski, S. Grabtchak, M. Ibisate, S. John, S. W. Leonard, C. Lopez, F. Meseguer, H. Miguez, J. P. Mondia, G. A. Ozin, J. Toader, and H. M. Van Driel, Nature (London) **405**, 437 (2000).
[2] M. Ghulinyan, C. J. Oton, G. Bonetti, Z. Gaburro, and L. Pavesi, J. Appl. Phys. **93**, 9724 (2003).
[3] J. Schilling, J. White, A. Scherer, G. Stupian, R. Hillebrand, and U. Gösele, Appl. Phys. Lett. **86**, 011101 (2005).
[4] D. A. Mazurenko, R. Kerst, J. I. Dijkhuis, A. V. Akimov, V. G. Golubev, D. A. Kurdyukov, A. B. Pevtsov, and A. V. Sel'kin, Phys. Rev. Lett. **91**, 213903 (2003).
[5] H. W. Tan, H. M. van Driel, S. L. Schweizer, R. B. Wehrspohn, and U. Gösele, Phys. Rev. B **70**, 205110 (2004).
[6] T. V. Dolgova, A. I. Maidykovski, M. G. Martemyanov, A. A. Fedyanin, O. A. Aktsipetrov, G. Marowsky, V. A. Yakovlev, and G. Mattei, Appl. Phys. Lett. **81**, 2725 (2002).
[7] M. G. Martemyanov, E. M. Kim, T. V. Dolgova, A. A. Fedyanin, O. A. Aktsipetrov, and G. Marowsky, Phys. Rev. B **70**, 073311 (2004).
[8] P. K. Kashkarov, L. A. Golovan, A. B. Fedotov, A. I. Efimova, L. P. Kuznetsova, V. Y. Timoshenko, D. A. Sidorov-Biryukov, A. M. Zheltikov, and J. W. Haus, J. Opt. Soc. Am. B **19**, 2273 (2002).
[9] J. Diener, N. Künzner, D. Kovalev, E. Gross, V. Y. Timoshenko, G. Polisski, and F. Koch, Appl. Phys. Lett. **78**, 3887 (2001).
[10] J. Diener, N. Künzner, D. Kovalev, E. Gross, and F. Koch, J. Appl. Phys. **91**, 6704 (2002).
[11] V. Y. Timoshenko, L. A. Osminkina, A. I. Efimova, L. A. Golovan, and P. K. Kashkarov, Phys. Rev. B **67**, 113405 (2003).